

# Mechanical stability of the magnet girder assembly at the SSRF

Xiao Wang,<sup>a\*</sup> Liang Chen,<sup>b</sup> Zhongbao Yan,<sup>a</sup> Hanwen Du<sup>a</sup> and Lixin Yin<sup>a</sup>

Received 28 December 2007

Accepted 7 March 2008

<sup>a</sup>Mechanical Engineering Group, Shanghai Institute of Applied Physics, Chinese Academy of Science, PO Box 800-204, Shanghai 201800, People's Republic of China, and <sup>b</sup>Department of Automation, Donghua University, Shanghai 201620, People's Republic of China.  
E-mail: wangxiao73@gmail.com

Electron beam stability is very important for third-generation light sources, especially for the Shanghai Synchrotron Radiation Facility (SSRF), whose ground vibration is much larger than other light sources. The mechanical stability of the magnet girder assemblies (MGAs) in a storage ring is essential for electron beam stability and performance. In order to improve the mechanical stability of the R&D MGAs in the storage ring of the SSRF, the number of MGAs in each lattice cell has been modified from three to five, and the girder structure has been optimized. Vibration measurements have been performed on the modified MGA prototype (the longest and heaviest MGA in the cell) to investigate mechanical stability and the influence of cooling water on magnet vibration. Measurement results show that the modified MGA has improved the first eigenfrequency from 5.9 Hz in R&D time to 21.9 Hz in the lateral and 22.5 Hz in the vertical direction; it has a good mechanical stability performance compared with other third-generation light source projects; and the influence of cooling water on the magnet vibration is about 4%, less than that of the ground vibration.

© 2008 International Union of Crystallography  
Printed in Singapore – all rights reserved

**Keywords:** vibration; stability; optimization; cooling water.

## 1. Introduction

The Shanghai Synchrotron Radiation Facility (SSRF) is a future third-generation light source, which will comprise a 3.5 GeV electron storage ring, injected from a 150 MeV linac through a full energy 0.15–3.5 GeV booster synchrotron, and an initial complement of seven beamlines. The SSRF aims at providing powerful X-rays to the Chinese synchrotron radiation users in a variety of research fields (Zhao, 2002).

Electron beam stability for third-generation synchrotron light sources is one of the most important requirements (Bialowons *et al.*, 2006). Mechanical stability of the magnet girder assemblies (MGAs) in a storage ring is essential for electron beam stability and performance, since the mechanical vibrations can be amplified on the electron beam closed orbit by more than ten times by the quadrupole magnets (Zhang, 2000*a*). Relevant research has been widely performed at many third-generation light source projects, such as the ALS (Advanced Light Source, USA) (Leung, 1993), ESRF (European Synchrotron Radiation Facility, France) (Zhang, 2000*b*; <http://www.esrf.eu/UsersAndScience/Publications/Highlights/2000/machine/XS10.html>), BESSY-II (Germany) (Feikes, 1996), APS (Advanced Photon Source, USA) (Sharma, 2005), SPring-8 (Japan) (Tsumaki & Kumagai, 2001), TLS (Taiwan Light Source, Taiwan) (Wang *et al.*, 2000), AS

(The Australian Synchrotron, Australian) (McKinlay & Barg, 2006), SPEAR3 (USA) (Dell'Orco, 2000), DIAMOND (UK) (Huang & Kay, 2006), KEK (Japan) (Masuzawa *et al.*, 2004) *etc.*

For the SSRF, the mechanical stability problem deserves more attention because ground vibration at the SSRF site is much larger than at other light sources (Bialowons *et al.*, 2006). However, the R&D MGA prototype does not appear to have a good dynamic performance, having a low first eigenfrequency of 5.9 Hz (Wang *et al.*, 2004). In order to improve its mechanical stability, a new prototype, the longest and heaviest MGA in a cell, is re-designed and re-fabricated after structure optimization. Here, vibration measurements have been performed on the modified MGA prototype to investigate the mechanical stability. Comparisons have also been made with other third-generation light sources. Finally, measurements have also been conducted to study the influence of cooling water on magnet vibration.

For the vibration measurements, we use a DH5920 data acquisition system from Jiangsu Donghua Measurement Technology (China) and 941-B seismometers from the Institute of Engineering Mechanics, China Earthquake Administration, with a sensitivity of 23 V m<sup>-1</sup> s and a frequency range of 1–100 Hz (Yang, 2001). The signal processing fundamentals were based on Zhou (2005). The displacement noted in the

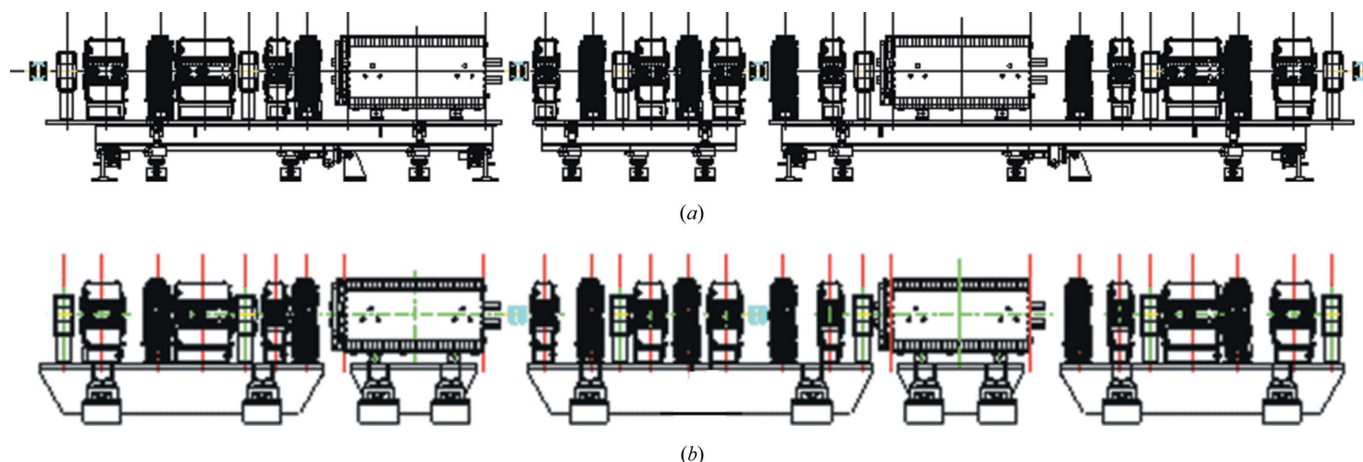


**Figure 1**  
Cell MGAs in (a) R&D, (b) modification.

measurement results is the root mean square (RMS) displacement.

## 2. Structure of the cell MGAs

### 2.1. In R&D

The SSRF storage ring is 432 m in circumference and consists of 20 similar cells. In the R&D period, each cell was designed to have three MGAs (shown in Fig. 1a), one short and two long. The short MGA is about 2 m long, with two quadrupoles, two sextupoles, one corrector magnet and a vacuum chamber. The long MGA is about 5.8 m long, with one dipole, four quadrupoles, three sextupoles, two corrector magnets and a vacuum chamber. The whole load is about 20.5 tons with 16.5 ton magnets on it. Fig. 2(a) shows the long MGA prototype. The girder has a box structure welded from steel plates of thickness 30–50 mm. The alignment system adopts the ‘six-strut’ support system, which has been used in other third-generation light sources, such as ALS.

The first eigenfrequency is an important index for the stability and performance of the MGAs. However, the R&D MGA prototype has a relatively low value compared with other third-generation light sources, which motivates us to take measures to improve it.

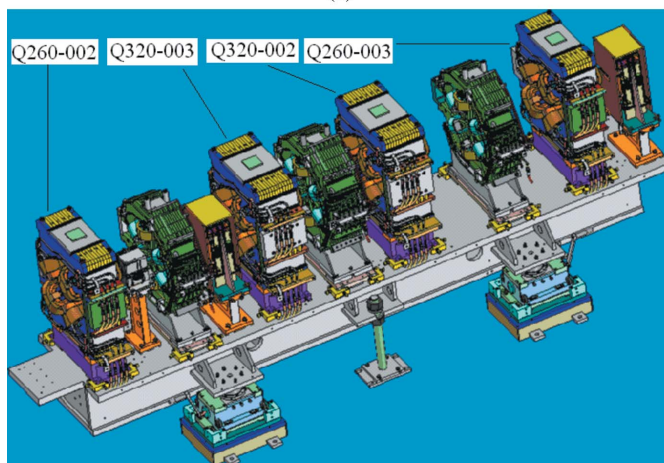
### 2.2. In modification

Through structure optimization, we make the following modifications for the cell MGAs.

(i) In every lattice cell, the number of MGAs has been changed from three to five, with each of the two dipole magnets having their own girders (shown in Fig. 1b). The whole load has been reduced by more than a half, and the whole length has been decreased by a third. It is easy to understand that such modifications are favourable for mechanical stability. The MGA in the middle is the heaviest and longest, with dimensions 4100 mm long, 800 mm wide and 590 mm high, weighing 8.8 tons including 6.0 ton magnets. The middle MGA has four quadrupoles, three sextupoles and two



(a)



(b)

**Figure 2**  
MGA prototype in (a) R&D, (b) modification.

corrector magnets (shown in Fig. 2b). The quadrupoles Q260-002 and Q260-003 are mounted on both sides, and Q320-003 and Q320-002 are mounted between them. The adjustment range is  $\pm 7$  mm in the vertical direction and  $\pm 10$  mm in the horizontal direction.

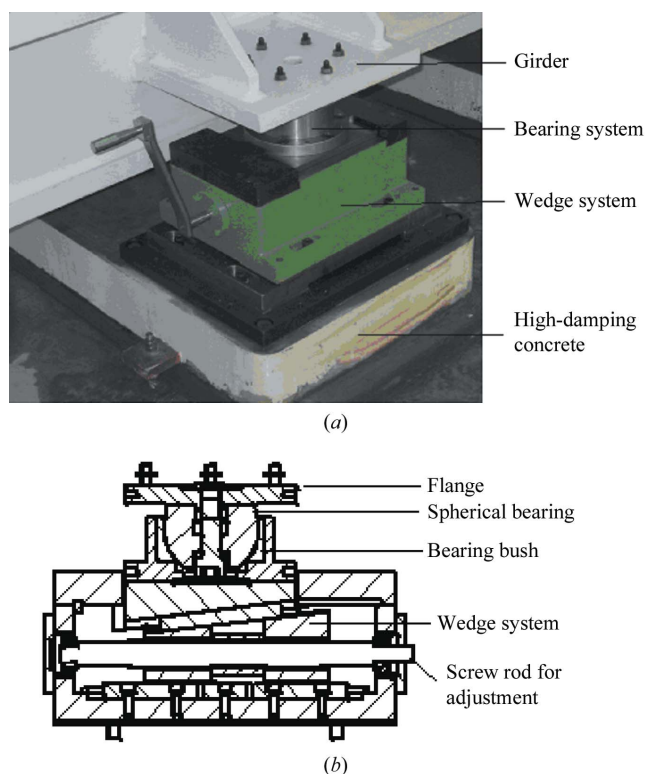


**Figure 3**  
Alignment system of the girder: (a) photograph, (b) cross section.

(ii) Wedge jacks are used in the alignment system, which includes a bearing system and a wedge system (see Fig. 3). In the bearing system, the diameter of the spherical bearing is 100 mm. In the wedge system, three directions can be adjusted by screw rods. Wedge jacks are connected to the girder body by flanges.

(iii) The bearing system is a crucial assembly in the design and fabrication of girders. The difficulty in its machining process is in the fit between the spherical bearing and the bearing bush. If the fit is too tight, good contact between components of the alignment system is difficult to maintain for small ground settlements; if the fit is too loose, the position of the magnets on the girder will easily drift owing to external forces. Thus, the mechanical requirements for the bearing systems are as follows: on the one hand, the spherical bearing can be rotated around the bearing bush under the weight of the MGAs; on the other, the contact surface should be retained as large as possible to assure sufficient stiffness for all the MGAs. An interference fit has been designed in order to obtain the rotation of the bearing bush only when the external moment exceeds 16 N m. Under the heavy burden of the magnet and the girder, the spherical bearing can rotate  $7^\circ$  in any direction to retain good contact with the bearing bush when the light source is at work.

(iv) The structure of the middle MGA is optimized by finite-element analysis (Wang, 2005), and high-damping concrete (shown in Fig. 3a) is used with a damping ratio twice that of normal concrete (Wang, 2006).

These modifications are favourable for mechanical stability of the MGAs.

### 3. Measurement results on the modified MGA prototype

Dynamic measurements on the R&D long MGA prototype were conducted at Shanghai Jiaotong University in 2001 (Wang *et al.*, 2004). Iron blocks with the same weight and center of gravity were used as substitutes for the corresponding magnets as there were not enough magnets fabricated at that time. Results show that the first eigenfrequency of the prototype is 5.9 Hz in the lateral direction. No response plots, such as spectra of displacement power spectrum density (PSD), transmissibility, were obtained at the same time.

In 2007, dynamic measurements were performed on the modified middle MGA prototype. It is obvious that the stiffness of this MGA is the weakest in the cell because it is the heaviest and longest. For a thorough investigation, the measurements are made for two cases.

#### 3.1. Measurement I

This case is intended to compare the vibration between the magnet, vacuum chamber, girder and floor. During the measurement, four sets of seismometers are put on the upper surface of the magnet Q320-003, the vacuum chamber, the girder and the floor. Each set consists of two seismometers, one for the lateral direction and the other for the vertical direction. Data are derived simultaneously from the four positions.

Fig. 4 shows spectra of displacement PSD, transmissibility and coherence. Here, transmissibility is the amplification ratio of the displacement of the vibration system to the floor displacement, and coherence represents the contribution of the floor vibration to the system vibration. The PSD and transmissibility plots (Figs. 4a–4d) for the lateral and vertical displacements show peaks at natural frequencies, 21.9 and 22.5 Hz, respectively, which correspond to the first eigenfrequencies calculated in these two directions. However, plots of the vacuum chamber also peak at 35 Hz in the lateral and 33 Hz in the vertical directions. These peaks are assumed to be due to the vacuum chamber support system. From Figs. 4(e) and 4(f) we can see that the coherence value is almost above 0.8 when below the first eigenfrequency. This means that, in this frequency range, vibration of the magnet and the vacuum chamber is caused by ground vibration in the same direction. However, as the frequency increases, the coherence value drops abruptly. This indicates that, in this frequency range, vibration of the magnet and the vacuum chamber is not only caused by ground vibration in the same direction but also by ground vibration in different directions.

Table 1 gives detailed measurement results, where the  $Q$  value is defined as the peak value in the transmissibility curve at the first eigenfrequency (Zhang, 2000). Since, as yet, there is no uniform criterion on the frequency range in the light source field, we adopt two bands: 4–50 Hz as suggested by Mangra & Sharma (1996) and 2–50 Hz for later use. From Table 1 we can see that in the lateral direction the girder-to-floor, vacuum-chamber-to-floor and magnet-to-floor displacement magnifications in the 4–50 Hz band are 1.13, 1.26 and 1.29, respec-

**Table 1**

Results in measurement I.

Measurement time (6 March 2007): day 15:41:11–16:01:11; night 22:01:12–22:21:12.

		Lateral				Vertical			
		Day		Night		Day		Night	
Frequency range (Hz)		2–50	4–50	2–50	4–50	2–50	4–50	2–50	4–50
Floor	Displacement (nm)	81.1	19.5	49.5	11.9	18.8	52.5	79.5	14.9
Girder	Displacement (nm)	88.1	22.1	54.8	13.5	18.9	52.6	80.4	15.0
	Ratio	1.09	1.13	1.11	1.13	1.00	1.00	1.01	1.02
	$Q$ value	11.9		10.3		1.8		1.1	
Vacuum chamber	Displacement (nm)	87.6	24.6	53.1	14.6	19.0	54.1	80.5	15.5
	Ratio	1.08	1.26	1.07	1.23	1.00	1.03	1.01	1.04
	$Q$ value	35.3		25.3		5.7		5.8	
Magnet	Displacement (nm)	89.8	25.2	55.2	14.9	19.9	55.2	84.4	15.7
	Ratio	1.11	1.29	1.12	1.25	1.06	1.05	1.06	1.05
	$Q$ value	34.8		28.2		1.6		1.1	

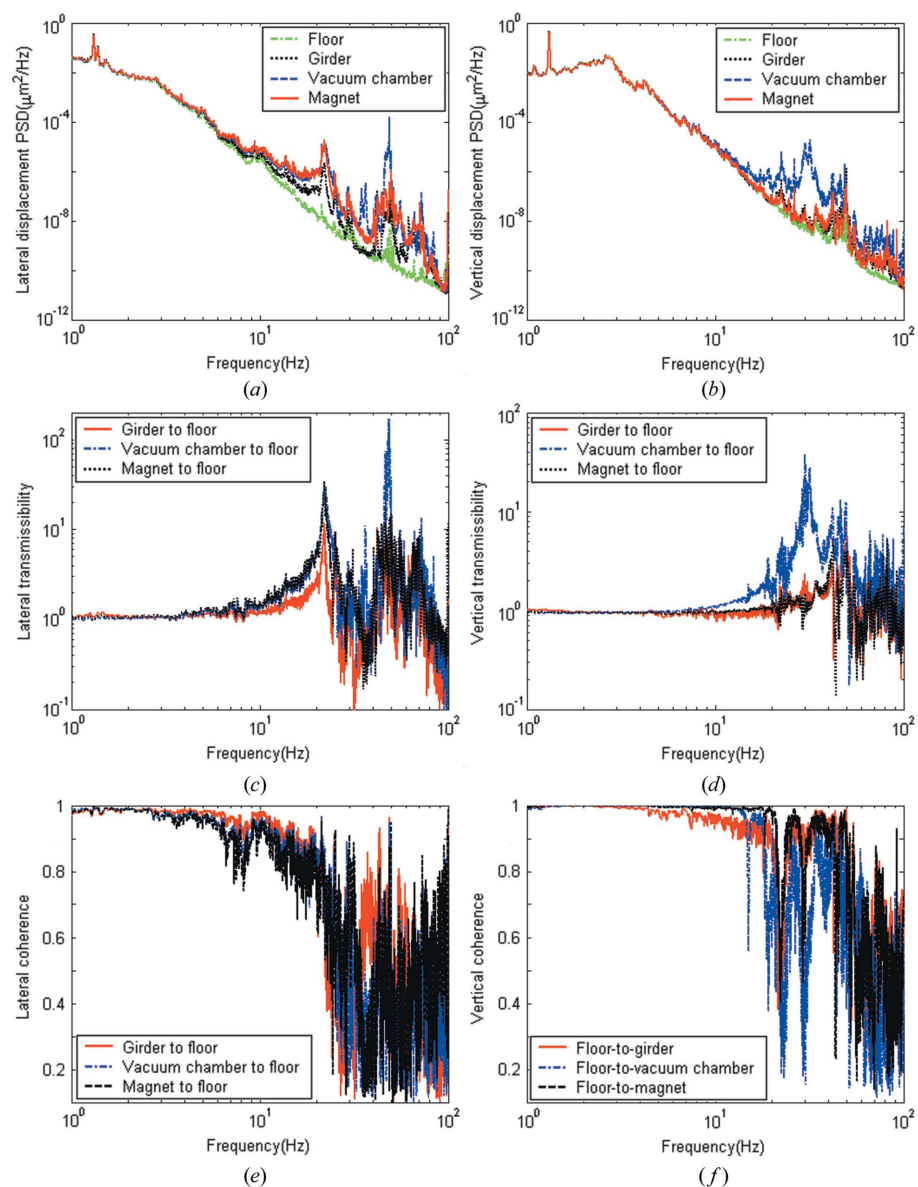


**Figure 4**

Results in measurement I: (a) lateral PSD, (b) vertical PSD, (c) lateral transmissibility, (d) vertical transmissibility, (e) lateral coherence and (f) vertical coherence.

tively; the  $Q$  values of the vacuum chamber, the magnet and the girder are 35.3, 34.8 and 11.9, respectively. These results show that vibration of the vacuum chamber and the magnet is much larger than that of the girder. In the vertical direction the displacement magnifications are no more than 1.05 and the  $Q$  values are no more than 1.8, except that of the vacuum chamber. These results indicate that vibration in the vertical direction is much smaller. In addition, the  $Q$  values and displacement magnifications in the daytime differ, and are usually larger than those at night. A similar phenomenon has also been found at the Diamond Light Source, using a Mobilyzer analyzer for data acquisition and Geotech KS-2000 M sensors (1/60 s to 50 Hz) (Huang & Kay, 2006). This phenomenon may be explained by the influence of ground vibration in different directions on the magnet and the vacuum chamber.

**3.2. Measurement II**

This case is intended to compare the vibration between different quadrupoles and the floor. During the measurement, five sets of seismometers are put on the upper surface of the magnets Q260-002, Q320-003, Q320-002, Q260-003 and the floor. Each set consists of two seismometers, one for the lateral direction and the other for the vertical direction. Data are derived simultaneously from the five positions.

Fig. 5 shows spectra of displacement PSD and transmissibility. These plots for the lateral and vertical displacements show peaks at natural frequencies, 21.9 and 22.5 Hz, respectively, corresponding to the first eigenfrequencies in these two directions.

Table 2 lists detailed measurement values. We can see that in the lateral direction the Q260-002-to-floor, Q320-003-to-floor, Q320-002-to-floor and Q260-003-to-floor displacement magnifications in the 4–50 Hz band are 1.34, 1.29, 1.31 and 1.34, respectively; the  $Q$  values of Q260-002, Q320-003, Q320-002 and Q260-003 are 47.3, 35.1, 34.4 and 38.8, respectively. These results show that quadrupole vibration at each end is larger. In the vertical direction

**Table 2**  
Results in measurement II.

Measurement time (6 March 2007): 14:57:45–15:17:45.

Frequency range (Hz)		Lateral			Vertical	
		2–50	4–50	6.5–100	2–50	4–50
Floor	Displacement (nm)	81.4	18.8	5.3	163.1	39.0
Q260-002	Displacement (nm)	88.5	25.1	11.6	173.0	41.1
	Ratio	1.09	1.34	2.19	1.06	1.05
Q320-003	Displacement (nm)	87.6	24.2	10.3	163.5	39.7
	Ratio	1.08	1.29	1.94	1.00	1.02
Q320-002	Displacement (nm)	91.1	24.7	10.1	165.2	39.2
	Ratio	1.12	1.31	1.91	1.01	1.01
Q260-003	Displacement (nm)	93.5	25.1	10.8	164.2	40.0
	Ratio	1.15	1.34	2.04	1.01	1.03

the displacement magnifications are less than 1.05 and the  $Q$  values are less than 5.2. These results indicate that vibration in the vertical direction is much smaller.

In general, from the results of the two measurements noted above, we find that the lateral first eigenfrequency of the modified MGA has reached 21.9 Hz, far above that of the R&D (5.9 Hz). Structure optimization therefore has obviously had the required effect.

### 3.3. Mechanical stability comparison with other light sources

To understand further the performance of the modified MGAs, their mechanical stability is compared with other third-generation light source projects in terms of the following three important indexes: (i) the first eigenfrequency, (ii) the  $Q$  value and (iii) the ratio of the integrated RMS displacement between the magnet and the floor. The higher the value (i) and

**Table 3**  
First eigenfrequencies (Hz) of various third-generation light source projects.

Project	First eigenfrequency	Project	First eigenfrequency
BESSY-II	5.6	DIAMOND	16.3
ALS	6.4	SPEAR3	17.2
ESRF	6.9	AS	17.3
APS	9.5	SPring-8	18.9
KEK	13.0	SSRF (R&D)	5.9
TLS	15.0	SSRF (modification)	21.9

**Table 4**  
 $Q$  values of various third-generation light source projects.

Project	Without damping devices	With damping devices	Damping devices
AS†	43.2	7.4	Damping plates
SSRF	47.3		
ESRF	50	10	Damping links
TLS	50	12	Damping pads
APS	100	10	Damping pads

† For the dipole girder.

the lower the values (ii) and (iii), the better the mechanical stability of the MGAs.

(i) The first eigenfrequency. The first eigenfrequencies of MGAs in various third-generation light source projects are listed in Table 3, from which we can see that the modified MGAs of the SSRF have a higher value.

(ii) The  $Q$  value. Table 4 gives  $Q$  values of MGAs in various third-generation light sources. We can see that the SSRF has a comparable value. Certainly, with increasing requirement for mechanical stability, various damping measures (see Table 4) have been taken to attenuate ground vibration and have achieved good effects.

(iii) Ratio of integrated RMS displacement. Table 5 gives lateral RMS displacement data of the ground and magnet vibration at various third-generation light sources. For the SSRF, daytime measurement results of quadrupole Q260-002 are used because this has the largest vibration amplitude as discussed above. No data in the vertical direction are listed because they cannot be found in formal publications. From Table 5 we can see that in the 2–50 Hz band the magnet-to-ground displacement magnification at the SSRF is only 1.15, the lowest in Table 5. This may be just a reference value because the ground vibration of the SSRF is relatively large. However, even when we consider the ratio of 1.34 in the 4–50 Hz band, it is still the lowest for the cases

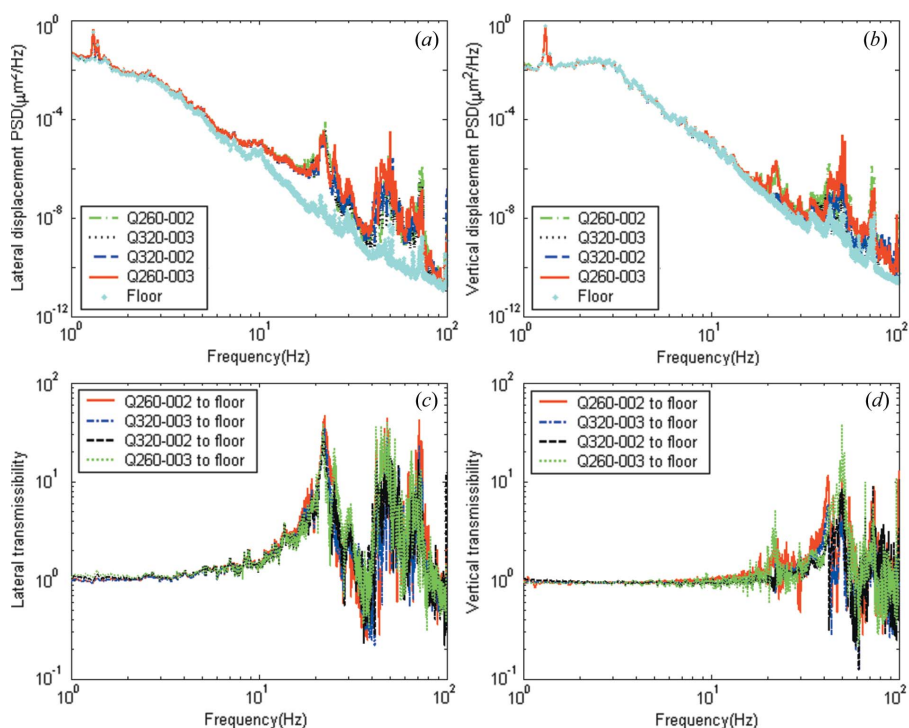


**Figure 5**  
Results in measurement II: (a) lateral PSD, (b) vertical PSD, (c) lateral transmissibility and (d) vertical transmissibility.

without using damping devices, and relatively small for the cases using damping devices in the 2–50 Hz band. Besides, in the 6.5–100 Hz band, the ratio of the SSRF (2.19) is smaller than that of AS with damping devices (2.53).

In general, the SSRF modified MGAs have relatively good mechanical stability. However, by considering the large ground vibration at the SSRF site, we should take further damping measures. Research on this aspect has been partly conducted (Wang *et al.*, 2006).

## 4. Measurement results with and without cooling water

To investigate the influence of cooling water on magnet vibration, measurements have been conducted on the quadrupole Q260-002 because it has the maximum vibration as discussed above. The flow velocity is  $1.77 \text{ m s}^{-1}$ , which coincides with the design criterion ( $1.5\text{--}2 \text{ m s}^{-1}$ ).

Fig. 6 shows spectra of transmissibility in the lateral and vertical directions. We can see that the curves with cooling water coincide with those without cooling water over the whole frequency range. This implies that the influence of cooling water on magnet vibration is small, which can be explained by the heavy weight MGA because the vibration amplitude is inversely proportional to the mass of the whole support (Redaelli *et al.*, 2002). When comparing Figs. 6(a) and 6(b), we find that the vertical transmissibility at the first eigenfrequency is much smaller than the lateral value.

Table 6 gives detailed measurement values in the lateral direction. We can see that the magnet-to-floor displacement magnifications are 1.28 without and 1.32 with cooling water. This means that the influence of cooling water on Q260-002 is only 4%. Besides, the ratio of the magnet vibration without and with cooling water is 1.11, and the ratio of the ground vibration is 1.08. This implies that magnet vibration is influenced by ground vibration more than by the cooling water. Similar conclusions can also be drawn from measurement results in the vertical direction.

It should be noted that these measurement results are just reference values because large installation activities were running about 40 m away during the measurements, which is not the operating environment of the SSRF.

## 5. Conclusion

In order to improve the mechanical stability of the SSRF R&D MGAs in the storage ring, we have changed the number of MGAs in each lattice cell from three to five and modified the girder by structure optimization. Vibration measurements have been performed on the modified MGA prototype to investigate the dynamic performance. The following conclusions can be drawn from the present analysis.

**Table 5**

Integrated RMS lateral displacement (nm) of various third-generation light source projects.

Project	Frequency range (Hz)	Without damping devices			With damping devices†		
		Ground	Magnet	Ratio	Ground	Magnet	Ratio
SSRF	2–50	81.4	93.5	1.15			
	4–50	18.1	25.1	1.34			
	6.5–100	5.3	11.6	2.19			
TLS	2–50	71	126	1.77	73	92	1.26
SPring-8	2–50	25	48	1.92			
ESRF	2–50	47	102	2.17	30	40	1.33
AS	6.5–100	6.3	21.4	3.40	4.9	12.4	2.53
BESSYII	2–315	150	500	3.33	150	250	1.67
APS	2–50	37	291	7.86	25	51	2.04
DIAMOND	1–100	14	134	9.57			
ALS	2–50	16	201	12.56			

† BESSY-II: damping plates, others are the same as those in Table 4.

**Table 6**

Lateral vibration influence of cooling water in the 4–50 Hz band (nm).

Measurement time (5 April 2007): 15:20:51–15:30:58 (without cooling); 15:43:20–15:53:42 (with cooling).

	Without cooling water	With cooling water	Ratio
Floor	25.1	27.1	1.08
Q260-002	32.2	35.7	1.11
Ratio	1.28	1.32	

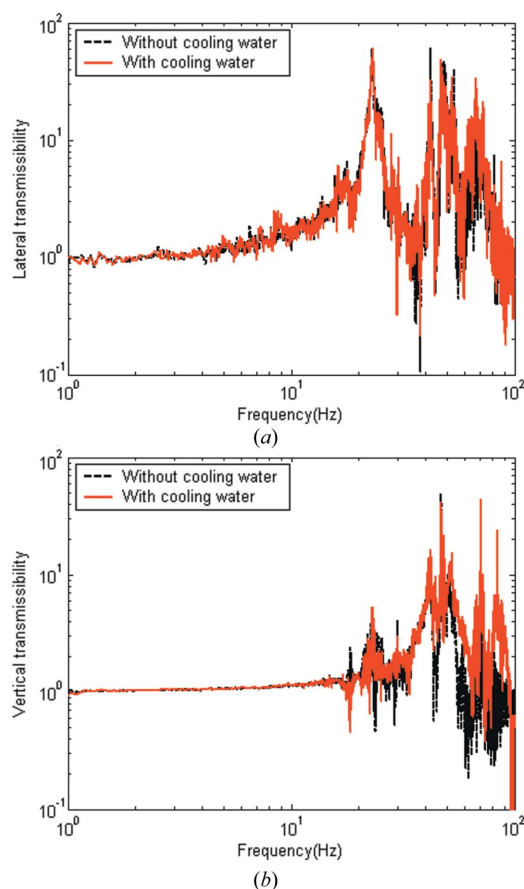


**Figure 6**

Measurement results with and without cooling water in (a) the lateral and (b) the vertical directions.

(i) For the R&D MGA prototype, the first eigenfrequency is only 5.9 Hz, which is small compared with other third-generation light sources.

(ii) For the modified MGA prototype, the first eigenfrequencies arrive at 21.9 Hz in the lateral and 22.5 Hz in the vertical directions; the  $Q$  values are 47.3 in the lateral and less than 5.2 in the vertical directions; the maximum ratios of the integrated RMS displacement are 1.15 in the 2–50 Hz band, 1.34 in the 4–50 Hz band and 2.19 in the 6.5–100 Hz band. All these values show that after structure optimization the SSRF modified MGAs have better mechanical stability, not only compared with the R&D MGAs, but also with various other third-generation light source projects.

(iii) The influence of cooling water on the magnet vibration of the modified MGA prototype is less than 4%. Magnet vibration is influenced by ground vibration more than by cooling water.

(iv) Some damping measures should be taken to further reduce the influence of ground vibration.

The authors would like to thank Ms Cuirong Wang and Mr Liankui Hao from Jiangsu Donghua Test Technology for their help in the modal measurements. They also thank the ME group of Shanghai Institute of Applied Physics, Chinese Academy of Science, for their assistance throughout the measurements.

## References

- Bialowons, W., Amirikas, R., Bertolini, A. & Kruecker, D. (2006). EUROTeV Report 2006-33, <http://www.eurotev.org/>.
- Dell'Orco, D. (2000). *22nd ICFA Workshop on Ground Motion in Future Accelerators*, SLAC, USA.
- Feikes, J. (1996). BESSY-II Internal Report. BESSY, Berlin, Germany.
- Huang, H. & Kay, J. (2006). *Proceedings of the Tenth European Particle Accelerator Conference (EPAC 2006)*, 26–30 June 2006, Edinburgh, Scotland, pp. 3338–3340.
- Leung, K. K. (1993). *Proceedings of the 1993 Particle Accelerator Conference (PAC 1993)*, 17–20 May 1993, Washington, DC, USA, pp. 1503–1505.
- McKinlay, J. & Barg, B. (2006). *International Workshop on Mechanical Engineering Design of Synchrotron Radiation Equipment and Instrumentation (MEDSI 2006)*, 24–26 May 2006, Hyogo, Japan.
- Mangra, D., Sharma, S. & Jendrzeczyk, J. (1996). *Rev. Sci. Instrum.* **67**, 3374.
- Masuzawa, M., Ohsawa, Y., Sugahara, R. & Yamaoka, H. (2004). *8th International Workshop on Accelerator Alignment (IWAA 2004)*, 4–7 October 2004, Geneva, Switzerland.
- Redaelli, S., Abmann, R. W., Coosemans, W. & Schnell, W. (2002). *Proceedings of the Eighth European Particle Accelerator Conference (EPAC 2002)*, Paris, France, pp. 485–487.
- Sharma, S. (2005). *Workshop on Ambient Ground Motion and Civil Engineering for Low-Emitance Electron Storage Ring*, Hsinchu, China.
- Tsumaki, K. & Kumagai, N. (2001). *Proceedings of 2001 Particle Accelerator Conference (PAC 2001)*, 18–22 June 2001, Chicago, IL, USA, pp. 1482–1484.
- Wang, D. J., Perng, S. Y., Chen, S. J. & Lin, C. J. (2000). *1st International Workshop on Mechanical Engineering Design of Synchrotron Radiation Equipment and Instrumentation (MEDSI 2000)*, 13–14 July 2000, Villigen, Switzerland.
- Wang, X. (2005). *FEA results of SSRF girders*. SSRF Internal Report. SSRF, Shanghai, People's Republic of China.
- Wang, X. (2006). *Dynamic test for the polymer concrete*. SSRF Internal Report. SSRF, Shanghai, People's Republic of China.
- Wang, X., Bu, L. S., Du, H. W. & Yan, Z. B. (2006). *International Workshop on Mechanical Engineering Design of Synchrotron Radiation Equipment and Instrumentation (MEDSI 2006)*, 24–26 May 2006, Hyogo, Japan.
- Wang, X., Yan, Z. B., Du, H. W., & Yin, L. X. (2004). *International Workshop on Mechanical Engineering Design of Synchrotron Radiation Equipment and Instrumentation (MEDSI 2004)*, 24–27 May 2004, ESRF, France.
- Yang, X. S. (2001). *Measurement Instrument and Techniques in Engineer Vibration, China measurement publications*, pp. 196–200.
- Zhang, L. (2000a). *22nd Advanced ICFA Beam Dynamics Workshop on Ground Motion in Future Accelerators*, Stanford, CA, USA.
- Zhang, L. (2000b). *Seventh European Particle Accelerator Conference (EPAC 2000)*, 26–30 June 2000, Vienna, Austria, pp. 2489–2491.
- Zhao, Z. T. (2002). *Nucl. Sci. Technol.* **13**, 168–172.
- Zhou, H. M. (2005). *Process Techniques of Test Signal, Publication of Beijing University of Aeronautics and Astronautics*, pp. 200–205.